MIMO Characterization on System Level of 5G Micro Base Stations Subject to Ran-domness in LOS

IEEE Access
The journal for rapid open access publishing

SPECIAL SECTION ON 5G WIRELESS TECHNOLOGIES: PERSPECTIVES OF THE NEXT GENERATION MOBILE COMMUNICATIONS AND NETWORKING

Received July 15, 2014, accepted August 21, 2014, date of publication September 18, 2014, date of current version September 25, 2014.

Digital Object Identifier 10.1109/ACCESS.2014.2358937

MIMO Characterization on System Level of 5G Microbase Stations Subject to Randomness in LOS

PER-SIMON KILDAL[1], (Fellow, IEEE), XIAOMING CHEN[1,2], MATTIAS GUSTAFSSON[3], AND ZHENGZHAO SHEN[3]

[1]Department of Signals and Systems, Chalmers University of Technology, Gothenburg 412 96, Sweden
[2]Qamcom Research and Technology AB, Gothenburg 412 85, Sweden
[3]Huawei Technologies Sweden AB, Gothenburg 40591, Sweden

Corresponding author: P.-S. Kildal (per-simon@kildal.se)

This work was supported in part by Huawei Technologies Sweden AB, Kista, Sweden, and in part by the Chalmers University of Technology, Gothenburg, Sweden.

ABSTRACT Wireless systems have become more and more advanced in terms of handling the statistical properties of wireless channels. For example, the 4G long term evolution (LTE) system takes advantage of multiport antennas [multiple-input multiple-output (MIMO) technology] and orthogonal frequency division multiplexing (OFDM) to improve the detection probability of single bitstream by diversity in the spatial and frequency domains, respectively. The 4G system also supports transmission of two bitstreams by appropriate signal processing of the MIMO subchannels. The reverberation chamber emulates according to previous works rich isotropic multipath (RIMP) and has proven to be very useful for characterizing smart phones for LTE systems. The measured throughput can be accurately modeled by the simple digital threshold receiver, accounting accurately for both the MIMO and OFDM functions. The throughput is equivalent to the probability of detection (PoD) of the transmitted bitstream. The purpose of this paper is to introduce a systematic approach to include the statistical properties of the user and his or her terminal, when characterizing the performance. The user statistics will have a larger effect in environments with stronger line-of-sight (LOS), because the angle of arrival and the polarization of the LOS contribution vary due to the user's orientation and practices. These variations are stochastic, and therefore, we introduce the term random-LOS to describe this. This paper elaborates on the characterization of an example antenna in both RIMP and random-LOS. The chosen antenna is a wideband microbase transceiver station (BTS) antenna. We show how to characterize the micro-BTS by the PoD of one and two bitstreams in both RIMP and random-LOS, by considering the user randomly located and oriented within the angular coverage sector. We limit the treatment to a wall-mounted BTS antenna, and assume a desired hemispherical coverage. The angular coverages of both one and two bitstreams for the random-LOS case are plotted as MIMO-coverage radiation patterns of the whole four-port digital antenna system. Such characterizations in terms of PoD have never been done before on any practical antenna system. The final results are easy to interpret, and they open up a new world of opportunities for designing and optimizing 5G antennas on system level.

INDEX TERMS Micro base transceiver station (uBTS), rich isotropic multipath (RIMP), probability of detection (PoD), random line-of-sight (random-LOS).

I. INTRODUCTION

The 4th Generation (4G) mobile communication system, also referred to by the acronym LTE (Long Term Evolution), has become very flexible compared to previous systems by its advanced dynamic digital signal processing capability. This is enabled by using multi-port antennas at both the transmitting and receiving sides, and referred to as MIMO (Multiple Input Multiple Output) [1]. The estimated channel voltages received on every port are processed by Maximal Ratio Combining (MRC). For the SIMO (Single Input Multiple Output) case this corresponds to complex conjugate matching of the received voltage. For the case of a plane wave arriving at an array of identical elements located side-by-side, the MRC corresponds to a classical phase-steered radiation pattern pointing in the direction of arrival of the wave. However, mobile communication systems are not limited to this classical Line-Of-Sight (LOS) of a single arriving wave. The digital processing is in particular

advantageous in multipath environments, to counteract the severe time-varying fading of the received signal for moving users. Such fading causes outage (i.e. no reception) during periods of the time for moving users, and corresponding outage among many stationary users in the environment, when these are considered to be arbitrarily located in the environment. The digital MIMO processing reduces the outage probability by using what is referred to as antenna diversity when receiving a single bitstream, and in addition it can use spatial multiplexing to transmit two or more bitstreams. The LTE system can in addition reduce the outage probability by using OFDM (Orthogonal Frequency Division Multiplexing). This corresponds to MRC in the frequency domain. The operational frequency band is divided in a large number of subchannels. These are so close that groups of neighboring subchannels fade similarly, but differently from one group to the next. Thereby, several independently fading groups of subchannels are created, and MRC will give an improved reception compared to using only one channel with fading.

The present paper introduces a new method to characterizing wideband micro base transceiver stations (BTS) on system level, applicable to the LTE systems and beyond. Micro BTS are base stations for micro cells with typical coverage of between 10 m and 100 m from the micro base station location.

Normal macro base stations have much larger coverage ranges than micro BTS, typically in the order of kilometer or more, and they are normally located on masts or walls, above most of the nearby buildings. They are also designed to illuminate certain angular regions and with a down-tilt of the beam into the area with buildings [2], [3]. Inside the buildings area there are users with smart phones and other wireless devices being subject to the reflections and scattering (i.e. multipath) of the buildings and other ground-located objects. The micro BTSs are different in the sense that they are located between the buildings or even indoors, i.e. within the multipath region together with the users and their terminals [4]. Therefore, the wireless environment of micro BTSs resemble that of wireless user-held terminals, with the exception that the BTS antennas are in fixed locations rather than being arbitrarily distributed and oriented like the user terminals. In this sense, the BTS antenna locations resemble those of hot spots for the wireless local area networks (WLAN) [5]. These characteristics of hot spot and BTS antennas make their radiation patterns of less interest than for macro base station antennas, in the same way that it now is well accepted that the shapes of the radiation patterns of antennas of wireless terminals play a minor role when determining performance in multipath.

Macro base stations are characterized by their radiation patterns defining the coverage area both in azimuth (wide beam) and elevation (narrow down-tilted beam). The antennas on the user terminals cannot be characterized by their radiation patterns because of the arbitrariness of the user orientation and location, and because they are subject to multipath coming from many and arbitrary angles of arrival (AoA). Instead, they are better characterized by their total radiation efficiency and, in the case of multi-port antennas, by their total embedded element efficiencies seen at each port and the mutual coupling between these ports [6]. The mutual coupling is important [7] because it contributes both to the statistical correlations between the received voltages on the antenna ports in the random multipath environment [8] and to their embedded element efficiencies [9]. Thus, both efficiency and correlation affect the performance of small antennas on wireless user-terminals in multipath. In the same way, efficiency and mutual coupling between ports will affect performance of multi-port BTS antennas. The embedded element efficiency corresponds to the decoupling efficiency in large digital beam-forming arrays for future radio telescopes [10].

The reverberation chamber has since year 2000 been developed into an accurate and efficient tool for characterization of small multi-port antennas for wireless terminals as well as the wireless terminals themselves, including the signal processing algorithms and the receiver sensitivity, as overviewed in [11]. The reverberation chamber can be well understood in terms of basic physics theories [12]. It emulates a rich isotropic multipath (RIMP) if it is well designed, and then we can perform measurements of all efficiency related quantities [6] and the accuracy is good [13]. Then, we can also uniquely obtain experimental results corresponding to the i.i.d. (independent and identically distributed) channel cases used in communication theory, provided the MIMO antennas have equal embedded element efficiencies on all ports, and that the ports are electromagnetically decoupled. The passive MIMO channel measurements in reverberation chamber are described in general terms in [6] and in details in [9], including definitions of diversity gains. The latest and most important developments relate to the measurement of throughput of LTE systems, for characterization of LTE devices. This is summarized in [11], which also shows that the measurements are in good agreement with basic theories for how MIMO diversity gain and OFDM work. These theories are based on the definition of an ideal digital threshold receiver [14], and they play an important role in the present paper in order to evaluate the probability of detection (PoD) of bitstreams, which we will use as the quality metric for the designed BTS antenna.

As already mentioned, micro BTS antennas are located inside the multipath environment together with the user and his wireless device. The BTS and the user may even be located in the very same room or hall. This means that there may be a significant LOS contribution to the wireless channel between them. We believe that this LOS contribution will be much more significant for BTSs than for terminals having contact with macro base stations. The LOS contribution will in a mobile wireless system be random due to the arbitrary orientation and location of the user, and it is therefore herein referred to as a random-LOS. The name indicates that the LOS contribution also needs to be characterized in terms of its statistical performance, in the same way as fading due to multipath. This was discussed in [11] where it was proposed

to introduce both the RIMP and the random-LOS as reference environments. They are also limiting environments (or edge environments) in the sense that the real-life environment is neither RIMP nor pure LOS, but something in between, i.e., not necessarily rich and with some LOS in addition to a multipath. Still, it is advantageous to have such well defined reference environments, inside which we get unique results from quality assessments. The relation to real-life environment was in [15] formulated as a real-life hypothesis that states that *"if a wireless device works well in both RIMP and random-LOS, it will also work well in real-life environment"*. This real-life hypothesis needs to be tested, but we will preliminary take it for granted in order to progress faster.

We will in the present paper characterize micro BTS antennas in the two above-mentioned edge environments. We also think that including the random-LOS in the characterization is even more important for BTS antennas than for wireless devices. The reason is that BTS antennas almost always will have a LOS to the device (they will be in the same room), whereas the device itself can be used both in macro-cell (rarely LOS) and in microcell (often LOS). Also, we will assume that the real-life hypothesis is valid, thereby also anticipating the testing of the hypothesis to determine under which conditions it really is valid. The random-LOS has already been studied when applied to a mock-up of a terminal with two small antennas for a diversity system [16]. The main purpose of the present paper is to introduce the way to characterize MIMO antenna systems in random-LOS by means of the PoD of different number of bitstreams.

It should be clear from the above that the requirements to micro BTS antennas are strongly relaxed compared to macro base stations. Their requirements may be more comparable with that of small antennas for wireless terminals. However, we should be able to design much better micro BTS antennas than antennas for wireless terminals, because BTS antennas are not limited by the same severe miniaturization requirements as antennas for handheld wireless devices. There is more available space in a BTS. Therefore, we used the relaxed requirements of BTS antennas, to rethink small cell BTS antenna types and construct an antenna that is much more compact than an antenna for a macro base station, and much more wideband than both normal terminal antennas and base station antennas. And, we will show and discuss its performance in both RIMP and random-LOS, in order to ensure good performance in real-life situations.

A micro BTS antenna has similar statistical nature of its location as a WLAN antenna for Wi-Fi hot spots. The latter antennas are known to be rather arbitrary in shape, producing rather randomized radiation patterns when the platform and its surroundings are included [5]. We introduce good quality metrics for both RIMP and random-LOS. Thereby, it is possible to optimize antennas for micro BTS and Wi-Fi hot spots for improved performance.

In this work, we have chosen the self-grounded bowtie antenna [17] as the candidate for the optimum design and characterization. This bowtie antenna has a simple mechanical structure, and it works over wide bandwidth. It was originally used for single linear polarization, obtained by differential excitation of two single-ended ports, i.e. a balun (180° hybrid) is needed. The self-grounded bowtie antenna was the basis of the 4-port butterfly antenna in [18] that is designed for use in MIMO measurements in reverberation chamber. However, the butterfly antenna is not compact enough for use as a micro BTS antenna, so we instead chose the dual-polarized bowtie as described in [19], and we use it herein as a 4-port MIMO antenna by splitting the two differential ports into four single-ended MIMO ports. The frequency of interest in this project is 1.7–2.7 GHz.

Throughout the paper, we assume a MIMO system and we use ViRM-lab (Visual Random Multipath environment Laboratory) [20] as the simulation tool to study performance in RIMP and random-LOS. The performance of the antenna is characterized in terms of its diversity gains and detection probabilities in RIMP and random-LOS. The PoD of single bitstream follows the theories in [14], and multiple bitstreams are generated by using the Zero Forcing (ZF) algorithm as outlined in [21]. We choose to quantify the diversity gain relative to the ideal Rayleigh curve in dBR (dB Rayleigh) [16], and the detection probabilities at 95% level in dBiid, i.e., relative to the corresponding i.i.d. case [21], [22]. We will explain a few key concepts in the next section.

The paper is organized as follows: First, we present in Section II how we propose to characterize performance of a MIMO antenna system in terms of the cumulative distribution function (CDF) and PoD of the processed channel matrix, both for one bitstream and two bitstreams. In order to do this we need to repeat some textbook material for the i.i.d. case. Then, in Section III we describe the two reference environments, and we show in Section III how we can use the PoD of the i.i.d. case as a reference in order to quantify the performance, even for the Random-LOS case. In Section IV we present simulated PoD-related results versus frequency for the wideband example BTS antenna. Finally we verify the results with measurements for the RIMP case, and explain how it has been done also for Random-LOS case.

II. DIVERSITY GAIN AND SPATIAL MULTIPLEXING BY MIMO

A. DIVERSITY GAINS IN *d*BR

Diversity gain is defined as the signal power improvement of the CDF of the diversity antenna output compared with that of a single ideal reference antenna at 1% level [8], [15]. This means that it is the improvement of the level received by the 1% worst cases or users during a fading cycle, when the transmitted power is the same. With ideal reference antenna we mean that the antenna has 100% total radiation efficiency. In practice this will be an antenna with known total radiation efficiency, and then we correct the reference level with this known efficiency. Apparent diversity gain is the diversity gain relative to the channel on the best antenna port, therefore

TABLE 1. i.i.d. diversity gains in dBR for MRC at three different CDF levels (well known values included for reference only).

CDF level	*2-port*	*3-port*	*4-port*	*5-port*	*6-port*	*7-port*	*8-port*
1%	*11.8 dBR*	*16.3 dBR*	*19.1 dBR*	*21.0 dBR*	*22.5 dBR*	*23.6 dBR*	*24.6 dBR*
5%	*8.4 dBR*	*12.0 dBR*	*14.2 dBR*	*15.8 dBR*	*17.1 dBR*	*18.1 dBR*	*19.0 dBR*
10%	*7.0 dBR*	*10.2 dBR*	*12.2 dBR*	*13.6 dBR*	*14.8 dBR*	*15.7 dBR*	*16.5 dBR*

only accounting for correlations and efficiency differences between the ports. The effective diversity gain is the diversity gain relative to the ideal reference, i.e. the apparent diversity gain in dB plus the efficiency of the best port in dB (the latter being a negative dB value).

In RIMP the CDF of each single port will have Rayleigh shape. Therefore, it is convenient to introduce the descriptive unit dBR, i.e. dB relative to Rayleigh CDF, for both the apparent and effective diversity gains.

It is useful to know the maximum available diversity gains for different numbers of i.i.d. channels, to have them as references. These are shown in Table 1, and illustrated in Fig. 1a for the best diversity algorithm, which is MRC. MRC corresponds to complex conjugate field matching as explained in the introduction. Note that 1000 000 realizations have been used in these simulation for determining the i.i.d. diversity gain.

B. RELATIVE THROUGHPUT AND PROBABILITY OF DETECTION (PoD) OF SINGLE BITSTREAM

For the sake of completeness, we present here the equations for calculating the average throughput. The group error rate (GER) is known to go very abruptly from only errors (1) to no errors (0) for the additive white Gaussian noise (AWGN) channel case in digital communication systems, and therefore we defined an ideal threshold receiver in [14], as

$$GER_{ideal}(P_0) = \begin{cases} 1, & P_0 < P_t \\ 0, & P_0 > P_t \end{cases} \tag{1}$$

where P_0 is the received power in the AWGN channel, and P_t is the threshold value. This definition makes it possible to find a very simple relation between the average throughput in a fading channel and the CDF of the received channels voltages, i.e.

$$T_{put}(P_{av}) = T_{put,\max}(1 - CDF(P_t/P_{av})) \tag{2a}$$

where $T_{put,\max}$ is the maximum achievable throughput, the *CDF* is the cumulative distribution function after the digital processing, and P_{av} is the average received power on the ideal reference antenna in the fading environment.

The simple relation between GER and throughput makes it possible to interpret the throughput as follows in a fading environment: *For the fading environment we do not know the instantaneous received power on each port, but we assume that we know the probability distribution of it as well as the average received power on a reference antenna with known total radiation efficiency. If the instantaneously received power is above the threshold, we will detect the channel with no errors, otherwise we will not detect it. Therefore, we can find the average throughput by counting the number of times the received power is above the threshold during the fading cycle, i.e. the number of detections of the channel, and the relative throughput is this number of detections divided by the total number of samples in one fading cycle. Thus, the relative throughput becomes equal to the probability of detection (PoD), i.e.*

$$PoD(P_{av}) = T_{put}(Pav)/T_{put,\max} = (1 - CDF(P_t/P_{av})) \tag{2b}$$

The PoD and the CDF are therefore closely related, as seen by comparing Figures 1a and 1b. The curves are the same except for the fact that the abscissa (in dB) and ordinate axes have been reversed, and in addition we prefer to use a logarithmic ordinate axis for the diversity gain. The diversity gain in dBR at 1% CDF level becomes identical to an improvement in dBR of the PoD at 99% level, and similarly for other CDF and PoD levels.

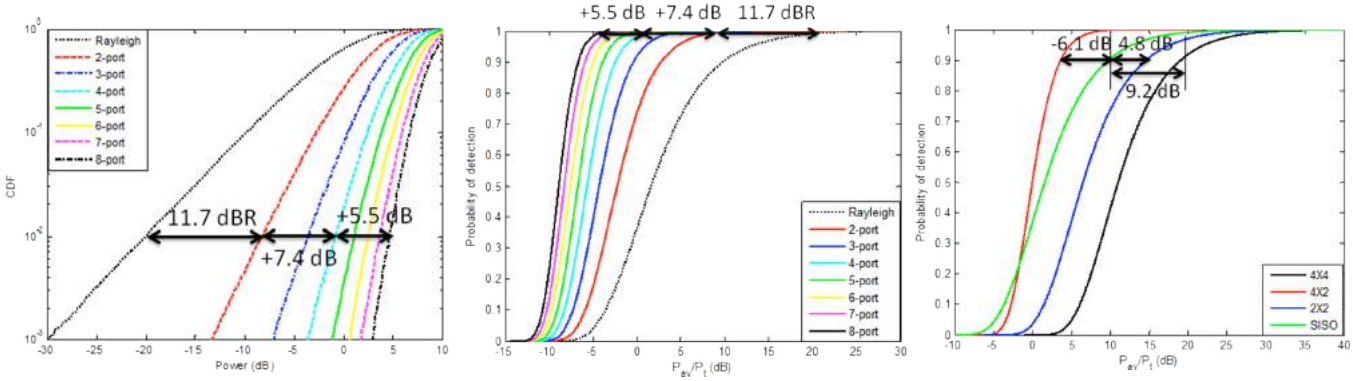

FIGURE 1. (a) CDFs of i.i.d. Rayleigh and different maximum ratio combining (MRC) outputs; (b) PoD for 1 stream of from several i.i.d. received channel using MRC; (c) PoD 1 stream, 2 streams and 4 streams in 1×1, 2×2, 4×2 and 4×4 MIMO systems, where the power cost of achieving higher order MIMO with respect to the 1×1 SISO case is marked at 90% PoD level. The curves shown are in principle textbook material, but they are included as reference curves for later use.

These relations between CDF, throughput and PoD have been proven for RIMP environments and we will here extend them to the random-LOS case.

C. PoD OF MULTIPLE BITSTREAMS BY ZERO FORCING (ZF)

We will now introduce the PoD of multiple bitstreams. We assume in this initial work that we have an open-loop, which means that there is no information about the channel at the transmitting side. We will also use the term bitstream or data stream or simply stream to denote the independent information-carrying modulated wave vectors that is coming in on each (or some) of the ports of the transmitting antenna via the transmission lines connected to their ports. We want to receive these bitstreams as separate independent streams after the digital processing on the receiving side so that we can extract the information in them. The two streams are intermixed on the output ports of the receiving antennas, so the digital processing is needed to separate them. There are several ways to do this, but we will here simply assume a Zero Forcing (ZF) algorithm. This algorithm does not require any knowledge about the Channel State Information (CSI), so there is no need for feedback from the receiving to the transmitting side, in contracts to the better Singular Value Decomposition (SVD) algorithm. We will now summarily explain how the ZF algorithm is working together with the threshold receiver as described in detail in [21] where it is also shown to provide agreement with throughput measurements on a commercial LTE device.

The threshold of the ideal digital receiver is not changed via the ZF transformations [24], and therefore the PoD of detecting all bitstreams will be equal to the PoD of detecting the weakest channel, i.e. the probability of $P_i > P_t$ for $i = 1, \ldots, N$, which is a function of P_{av} in the environment. Therefore, we evaluate this when using ZF algorithm. SVD is better because it performs smart beam steering also on the transmitting side, but this requires that full CSI is available in the receiver. SVD is not implemented in the LTE FDD system, but it is in principle possible in LTE TDD for which there is no need for feedback of the CSI because channel state is the same on both sides of the communication link. SVD will most probably be available in 5G. Still, SVD with CSI known only represents a constant improvement of the PoD curve in a RIMP environment of about 1.5 dB [23], so we will not treat the SVD in this initial work.

Fig. 1c shows the probability of detecting 1 bitstream, 2 bitstreams and 4 bitstreams in 1×1, 2×2, 4×2 and 4×4 MIMO systems using ZF. There is no CSI on the transmitting side, so it is assumed that the power is distributed equally between the ports on the transmitting side. The differences between the curves at 90%, 95% and 99% PoD levels are summarized in Table 2. These values represent the power cost for achieving higher order MIMO compared to the 1×1 SISO case and are included here as reference values although being well known.

TABLE 2. Power cost for achieving higher order MIMO with respect to the 1x1 SISO case for ZF algorithm.

	4×4	4×2	2×2
90% PoD	9.2 dB	-6.1 dB	4.8 dB
95% PoD	9.2 dB	-8.0 dB	4.8 dB
99% PoD	9.1 dB	-12.4 dB	4.8 dB

III. DESCRIPTION OF THE TWO EDGE ENVIRONMENTS RIMP AND RANDOM-LOS

In the introduction we gave a background to the RIMP and random-LOS edge environments, linked together by a real-life hypothesis. In RIMP environments, there are many incident waves and the angles of arrival of these waves are uniformly distributed over the whole unit sphere. We typically use 20 incident waves in our channel simulations with ViRM-lab, thereby ensuring convergence for normal not-directive radiation patterns. For each realization we redistribute the 20 waves.

In random LOS environments, there is only one incoming wave, so the scenario is pure-LOS but we prefer to refer to it as random-LOS due to the randomness of the location and orientation of the device. However, the angle of arrival is random relative to the antenna on the device when we include the arbitrary location and orientation of the user and his device. The simulations of the random-LOS performance are done in the same way as for RIMP, except that we use only one wave for each realization. We normalize the channel in the same way and for the same reason as for the RIMP case. Note that in random-LOS, we need to separate the cases for which the incident wave is linearly and circularly polarized, and we use the abbreviations LP and CP to denote linear and circular polarizations of the incoming wave, respectively.

When considering wireless user-terminals it is evident that the arbitrary orientation can be regarded as random in three dimensions (3D), with an AoA that is uniformly distributed over all directions in space (i.e. over a solid angle of 4π and with arbitrary polarization. This is in particular true for smart phones, which can be used with any edge of the screen upwards. However, a micro BTS will have a fixed location and orientation, and the orientation will most probably be the same for micro BTS stations located at different places, and, in particular if they have been installed by professional people and not by a public customer. In this work, we assume the wall-mounted scenario, i.e. the case when the antenna is mounted on a wall, and for which it is desirable to only illuminate one side of the wall, i.e. half-space.

We treat the wall-mounted case as a half-space 3D-random LOS, by arguing that 1) the user-terminal can be at any direction within the half-space relative to a coordinate system fixed to the micro BTS, i.e. the AoA is distributed uniformly over 2π, and that 2) the terminal is oriented arbitrarily so that for the LP case the incident wave can have any arbitrary linear polarization. We do not include the statistical level variation of the incident wave, so the statistics of the received voltage at each port of the BTS is limited to the variations caused

by its far field patterns at this port. We will treat linearly and circularly polarized incident waves separately, because we will need to know mainly the LP case as LP antennas are most common in wireless terminals, although we could easily have generated a completely arbitrary polarization and characterized for that case as well.

A. CORRELATION IN RIMP AND RANDOM-LOS

Correlation is a measure of the similarity of two random variables. A small correlation means that the two random variables will vary independently; a large correlation means the two random variables will vary similarly or with a constant ratio between them. We deal with complex correlations between complex channels (received port voltages). Small correlations give higher diversity gain than large ones, and the empirical relation between them is quite simple for 2-port antennas [25].

We can assure low correlation in RIMP either by:

a) *reducing the mutual coupling between the antenna ports, which is done by making them orthogonally polarized or having far fields radiating in different directions, or by*

b) *separating the antennas, because in RIMP the received voltages become almost uncorrelated by separations larger than typically 0.25 wavelengths.*

In a pure-LOS environment, we can also ensure uncorrelated outputs of the two antenna ports by the former method *a*. However, it does not help to separate the antennas, unless the separation is very large (it depends also on the distance to the transmitting side). Therefore, for micro base stations we have to rely on creating in some way orthogonal far field patterns by polarization or direction. The indirect measure of the quality is again the mutual coupling between the ports, because antennas that are orthogonal in polarization or direction have low mutual coupling. The direct measure of quality will be the location of the 90% or 95% level of the PoD relative to the receiver threshold or the corresponding i.i.d. level.

We will study the effect of correlation for the RIMP and random-LOS cases later during the characterization of the example bowtie antenna.

IV. QUANTIFYING PERFORMANCE IN RIMP AND RANDOM-LOS

A. THE i.i.d. CASE AS REFERENCE FOR DIVERSITY GAIN OF CDFs

The diversity gain in RIMP is equal to that of the i.i.d. case if the antenna ports have equal and 100% embedded element efficiency, and there is no correlation between the voltages on the ports. The latter is true if the ports are electromagnetically uncoupled in polarizations or radiation directions of their far fields, or located so far from each other that correlation is vanishing. The latter condition is in RIMP satisfied quite well already after a separation of a quarter of wavelength, at least for small dipole- or monopole-like antennas. When there is mutual coupling performance is deteriorated due to the total embedded element efficiency [6]. This corresponds to the so-called decoupling efficiency of a more general array design [10]. The mutual coupling will also degrade the correlation.

Thus, in RIMP the practical diversity gains will always be lower than those for the corresponding i.i.d. cases. Thus, we can refer to the quality of it in terms of a positive value in *dBR* that is lower than the maximum available ones in Table 1. Alternatively, we can characterize the quality in terms of a degradation of the CDF in *dBiid* at a certain probability level, i.e. relative to the CDF of the i.i.d. case.

The i.i.d. cases do not represent a theoretical limit of the performance in random-LOS. Still, it is convenient to quantify the performance of diversity gain in random-LOS in *dBR* or *dBiid*, in particular for small antennas for mobile terminals, which in practice has close to Rayleigh distributed CDFs in random-LOS [16]. Therefore, we will also use the Rayleigh distribution and the i.i.d. case as a reference for quantifying the random-LOS performance.

B. THE i.i.d. CASE AS REFERENCE FOR DIVERSITY GAIN OF PoD

In the same way we can measure the quality of a practically realized channel matrix in terms of the location of the PoD curve in *dBiid*, at a specific PoD level, for the number of bitstreams we want to receive, i.e. in dB relative to the corresponding i.i.d. curve. This quality will always be smaller than 0 dB for the RIMP case and can therefore also be called the MIMO bitstream efficiency.

C. THE HYPOTHETICAL SINGLE- AND DUAL-POLARIZED ISOTROPIC REFERENCES FOR RANDOM-LOS

The diversity gains in random-LOS have also a limitation like they have in RIMP, but this is not yet known except for what is studied in [23], and it is clear that the diversity gains in random-LOS may be larger than the diversity gain for the i.i.d. case. There is nothing unphysical in having a diversity gain for random-LOS that is larger than the i.i.d. case. Random-LOS is statistical due to the random AoA and polarization of the incident wave (from the user-terminal), and these two contributors do not cause enough randomness to ensure a Rayleigh distribution of each channel like in the i.i.d. case, and therefore the i.i.d. case does not represent the limit.

Let us here give a hypothetical example of a case for which it is easy to understand that the i.i.d. case is not a limit for the random-LOS diversity gain. Consider a two-port reference antenna with isotropic and orthogonally polarized embedded far field patterns. This means that each port receives arbitrarily polarized waves from any direction with the same probability. Therefore, when the two ports are MRC combined, they will dynamically match to the polarization of one arbitrarily polarized incident wave. Therefore, the two ports become together an ideal isotropic antenna that is polarization-matched to any incident wave. The two ports receive together two orthogonal arbitrarily polarized waves from any direction. We can separate these two received waves by linear operations on the wave voltages in such a way that

the total response of the antenna and the processor together becomes a diagonalization of the voltage matrix. Thus, this dual polarized isotropic antenna can receive orthogonal polarizations from any direction in space, and there is no statistical variation of the signal in random-LOS if the incoming wave has constant amplitude. Thus, the best possible antenna for random-LOS is this hypothetical antenna which has 0 dBi gain for any polarization in all directions. If the incident wave is CP and the two antenna ports LP, there is also no signal variation of the received signal on each port, so each port is already much better than Rayleigh fading. However, such isotropic antennas are not physical. Still convenient references in agreement with the isotropic reference we use for quantifying directivity in free space environments.

When presenting PoDs, the $P_{av}/P_t = 0$ dB line corresponds to the PoD of the dual-polarized 2-port isotropic reference antenna. This means that a 3-port isotropic antenna will have a step-like 1-stream PoD curve that change abruptly from zero to one at a level of $P_{av}/P_t = 2/3 = -1.8$ dB. A 6-port isotropic antenna with uncoupled ports this transition (step) will appear at $P_{av}/P_t = -4.8$ dB. This is the largest number of independent antenna ports that it is possible to realize on a small incremental volume [23].

V. DESIGN OF THE 4-PORT BOWTIE ANTENNA

The single-polarized self-grounded bowtie antenna was presented in [17]. We developed in parallel to the present project a dual-polarized version for the frequency range from 1.5 to 3 GHz [19], covering our desired frequency range with some margins. We use this here as a 4-port antenna by using each of the two opposite terminals of its two differential ports as individual single-ended ports. This represents also a simplification compared to the original dual-polarized bowtie, because we do not need any balun to use the 4-port version. We characterize it here as a 4-port wall-mounted micro BTS antenna for MIMO systems up to order 4×4. The final geometry is shown in Fig. 2.

We emphasized both size and good random-LOS performance during the modification of the EM design, in addition to manufacturability. The main issue was to reduce all S-parameters between the four ports. The resulting performance could have been better, but only by increasing size, which was not desirable. We later found out that we were dealing with a physical limitation on MIMO order related to the size of the antenna, see the discussion of this in the conclusion and in [23].

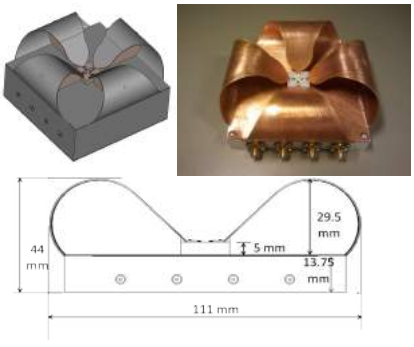

FIGURE 2. Drawing, photo and cross-section of the 4-port self-grounded bowtie antenna for 1.5–3 GHz. Each port excites one petal of the antenna, and the mutual coupling between the ports is low. All petals are connected to the rim of a common ground plane.

Fig. 3a shows the directivity of each element (i.e. petal) of the bowtie, as well as the direction at which this appears. The direction is given in degrees from the normal to the ground plane, and it appears in the symmetry plane of the excited petal, and in the same azimuthal direction from the normal as the petal is located. We see that the directivity varies between 3.7 and 5.3 dB over the desired frequency band, and the main beam direction is between 20° and 28° from the normal. The directivity of a Huygens source is 4.8 dB [23]. Therefore, the petals of the bowtie antenna radiate similar to the far field of four Huygens sources, with their main beams spread on a cone with cone-angle of approximately 25° around the normal to the ground plane.

A. COMPUTED S-PARAMETERS, CORRELATIONS IN RIMP AND EMBEDDED ELEMENT EFFICIENCIES

The S-parameters, correlations between port in RIMP environment, and total embedded radiation efficiencies of the 4-port bowtie antenna are shown in Fig. 3. The bowtie antenna is almost lossless, so the embedded element efficiencies [6] and the correlation in RIMP can be obtained from the S-parameters [26]. We see that all S-parameters are below −10 dB over most of the frequency band. This is normally sufficient to ensure high embedded element efficiency of a lossless antenna. Still, the embedded element efficiency is between −1 and −1.5 dB, which is quite low. The reason is that there are many ports. Also, the achieved correlation is small enough for good performance of a 2×2 diversity system, whereas it should have been lower to ensure optimum performance for the multiple bitstream cases, which are much more sensitive to correlation [21]. We managed to improve the embedded efficiency and correlation by separating the four ports. However, then the antenna became too large in size, so we decided to prioritize smaller size rather than better efficiency. As an example, the butterfly antenna in [18] has better performance, but it is too large for our micro BTS application. The butterfly antenna is also radiating on both sides of the ground plane, so it cannot be used wall-mounted.

B. DIVERSITY GAINS IN RIMP AND RANDOM-LOS

Fig. 4a shows the MRC diversity gain of the bowtie antenna in RIMP, computed by using ViRMlab. The correlation between any two ports is quite low, as previously observed in Fig. 3c. Still, the correlations between all the 4 ports have a large effect on the diversity gain. This is clearly seen on the apparent diversity gains (excluding the effect of the embedded radiation efficiency), from which it can be seen that the correlations together reduce the diversity gain by more than

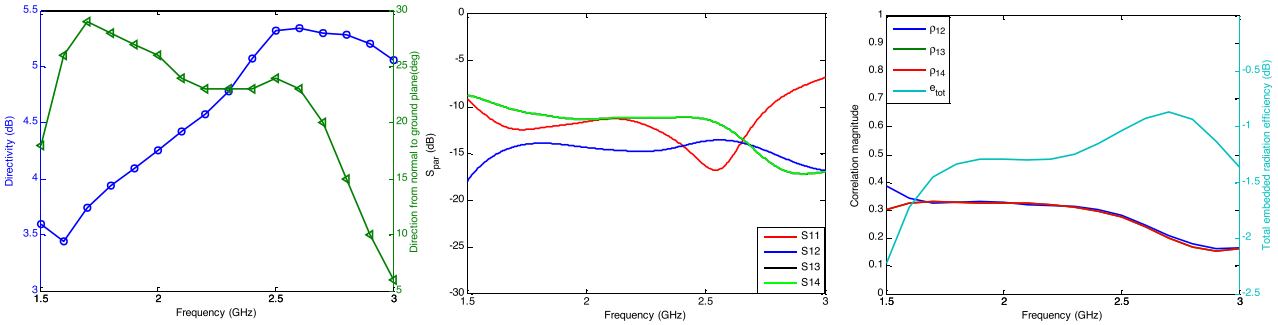

FIGURE 3. Computed performance of the 4-port bowtie antenna. (a) Maximum directivity at one of its port and its direction (in the symmetry plane) relative to the normal to its ground plane, (b) S-parameters, (c) correlation ρ between the different ports in RIMP and total embedded radiation efficiency e_{tot}.

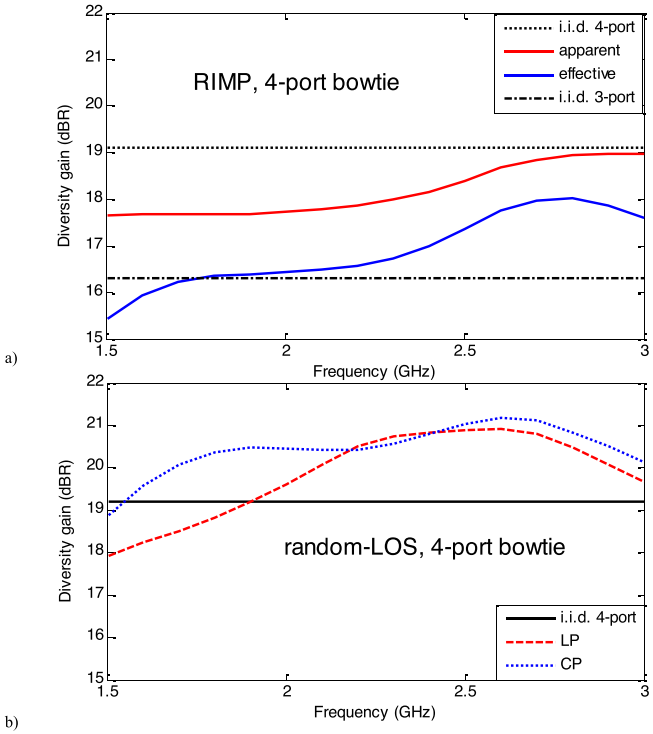

FIGURE 4. Computed diversity gains at 1% CDF of the bowtie antenna. (a) 4-port bowtie in RIMP; (b) 4-port bowtie in random-LOS for wall-mounted scenario. LP and CP denote linear and circular polarizations of the arriving wave in random-LOS, respectively.

1 dB at the low frequency end. We have also plotted the theoretical diversity gains for three and four i.i.d. channels in the two graphs. We see that the achieved diversity gains falls between these two limiting cases. We explain this with reference to [23], in which we show that in free space we cannot get more than 6 uncoupled antenna ports in an incrementally small volume. These 6 ports can be connected to three orthogonal electric and three orthogonal magnetic current sources, or they can be coupled to 6 orthogonal Huygens sources. The latter is a directive source with directivity of 4.8 dBi, quite close to the directivity seen at each port of the bowtie antenna. Each petal of the bowtie antenna radiates therefore close to a Huygens source, and we cannot have more than three independent such Huygens antennas radiating into half-space (6 radiating into full space). This represents a physical limitation when the multi-port antenna is small, such as in the lower part of the frequency band in our case. This makes it impossible to get larger diversity gains unless we increase the size of the antenna by separating each port and thereby petal, and we could not do that due to our size constraints.

The MRC diversity gain of the bowtie antenna in random-LOS for the wall-mounted case is shown in Figs. 4b. The diversity gains can be explained by looking at the MIMO-coverage patterns of the bowtie antenna, which will be presented and discussed in Sec. IV-D. We see in Figs. 4b that the diversity gain is larger than for the corresponding i.i.d. case. This is not unphysical because the i.i.d. case does not represent any upper bound for the random-LOS case, as discussed in Sec. IV-C.

C. PoD OF 2 AND 4 BITSTREAMS IN RIMP BY ZF ALGORITHM

The probability of detecting 2 and 4 streams in RIMP with ZF algorithm is shown in Fig. 5 for the 4-port bowtie antenna in 4×2 and 4×4 systems, respectively. The corresponding 2- and 4-stream MIMO efficiencies are shown in Fig. 6. We see that the 2 stream MIMO efficiencies are −5 dBiid, −3 dBiid and −1.5 dBiid at 90% PoD at the three frequencies 1.7, 2.2 and 2.7 GHz. The performance is better at high frequency because the correlation is lower there. This is much more pronounced for the 4 bitstream cases for which the MIMO 4 stream efficiencies at 90% PoD are −15 dBiid, −10 dBiid, and −3 dBiid at the three frequencies. This is because the smallest eigenvalue of the 4-port bowtie antenna is too small to support the 4th stream at low frequencies (e.g., the eigenvalues at 1.7 GHz are 0.0077, 1.3271, 1.3271, and 1.3381). Thus, it is difficult to get 4 bitstreams with the proposed compact 4-port bowtie in RIMP.

To get better performance we need a larger antenna due to the physical size limitation in [23]. In addition to the normal 4-port bowtie antenna, we differentially combine every two opposite ports of the bowtie antenna to obtain a 2-port bowtie antenna (i.e., differentially excited 2-port bowtie antenna). The 2-port bowtie antenna has embedded

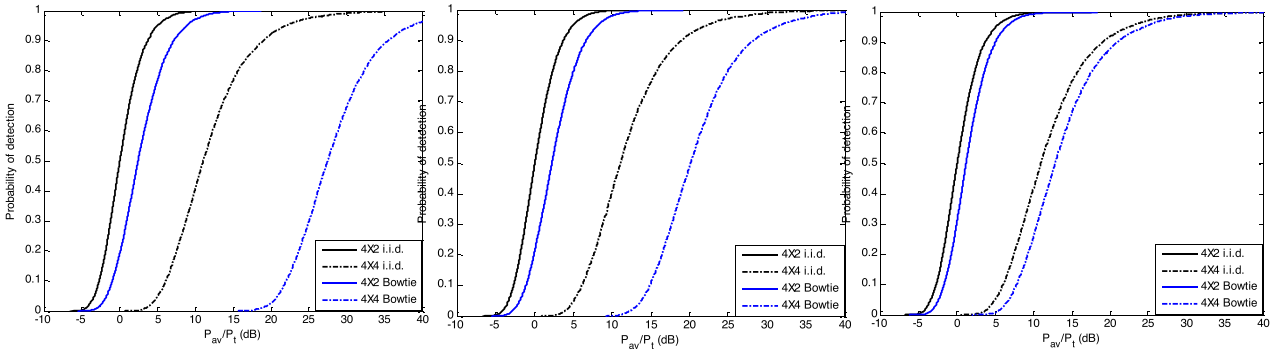

FIGURE 5. Probability of detection by ZF algorithm of 2 and 4 streams in RIMP of the 4-port bowtie antenna at 1.7 GHz, 2.2 GHz, and 2.7 GHz, from left to right.

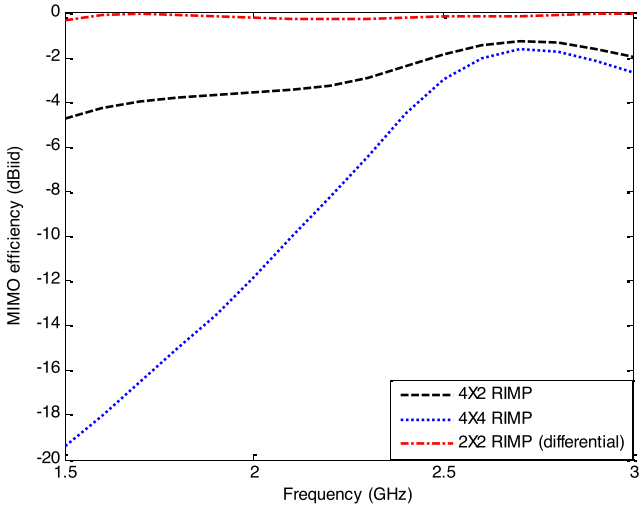

FIGURE 6. 2- and 4-stream MIMO efficiencies in dBiid at 95% PoD for the 4-port bowtie antenna and the differentially excited 2-port bowtie antenna in RIMP as a function of frequency. The i.i.d. reference for the M × N bowtie configuration is the M × N MIMO system for the i.i.d. case.

radiation efficiencies above −0.2 dB over the whole frequency range, in contrast to the low embedded efficiencies for the 4-port case (see Fig. 3d). Moreover, the two ports of the differentially exited 2-port bowtie antenna are orthogonally polarized, resulting in zero correlation. Because of these good properties, the MIMO efficiency of the differentially exited 2-port bowtie antenna (supporting 2 stream) is close to 0 dBiid, i.e., the MIMO performance of the differentially exited 2-port bowtie antenna is close to the i.i.d. case. Nevertheless, it should be pointed out that although the differentially exited 2-port bowtie antenna has good performance in RIMP, its spatial MRC coverage (and therefore random-LOS performance) is not as good as that of the normal 4-port bowtie antenna.

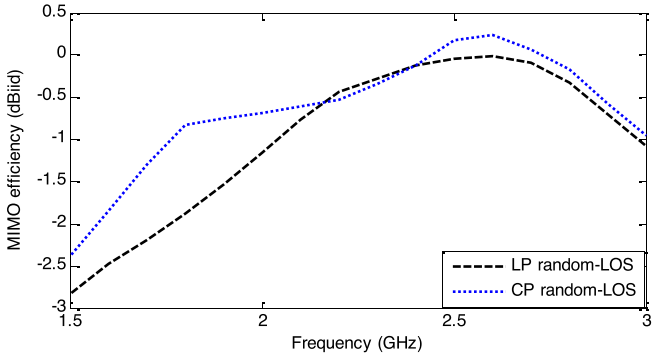

FIGURE 8. MIMO 2-stream efficiency at 95% PoD of the 4-port bowtie antenna for the wall-mounted scenario in random-LOS over half-sphere.

D. PoD OF 2 AND 4 BITSTREAMS IN HALF-SPACE RANDOM-LOS BY ZF ALGORITHM

Fig. 7 shows the probability of detecting two bitstreams using 2 and 4 ports of the bowtie antenna for the wall-mounted

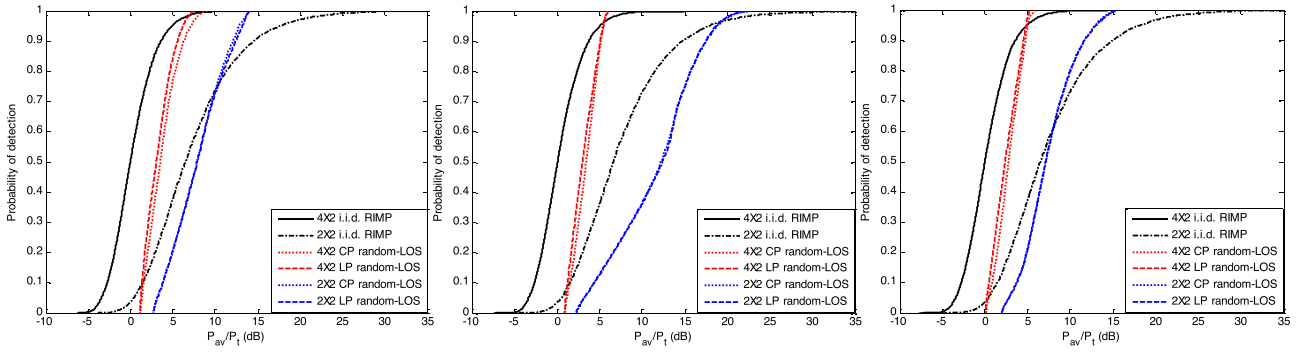

FIGURE 7. Probability of detecting two bitstreams for the wall-mounted scenario in random-LOS of the 2- and 4-port bowtie antenna at 1.7 GHz, 2.2 GHz, and 2.7 GHz, from left to right, respectively.

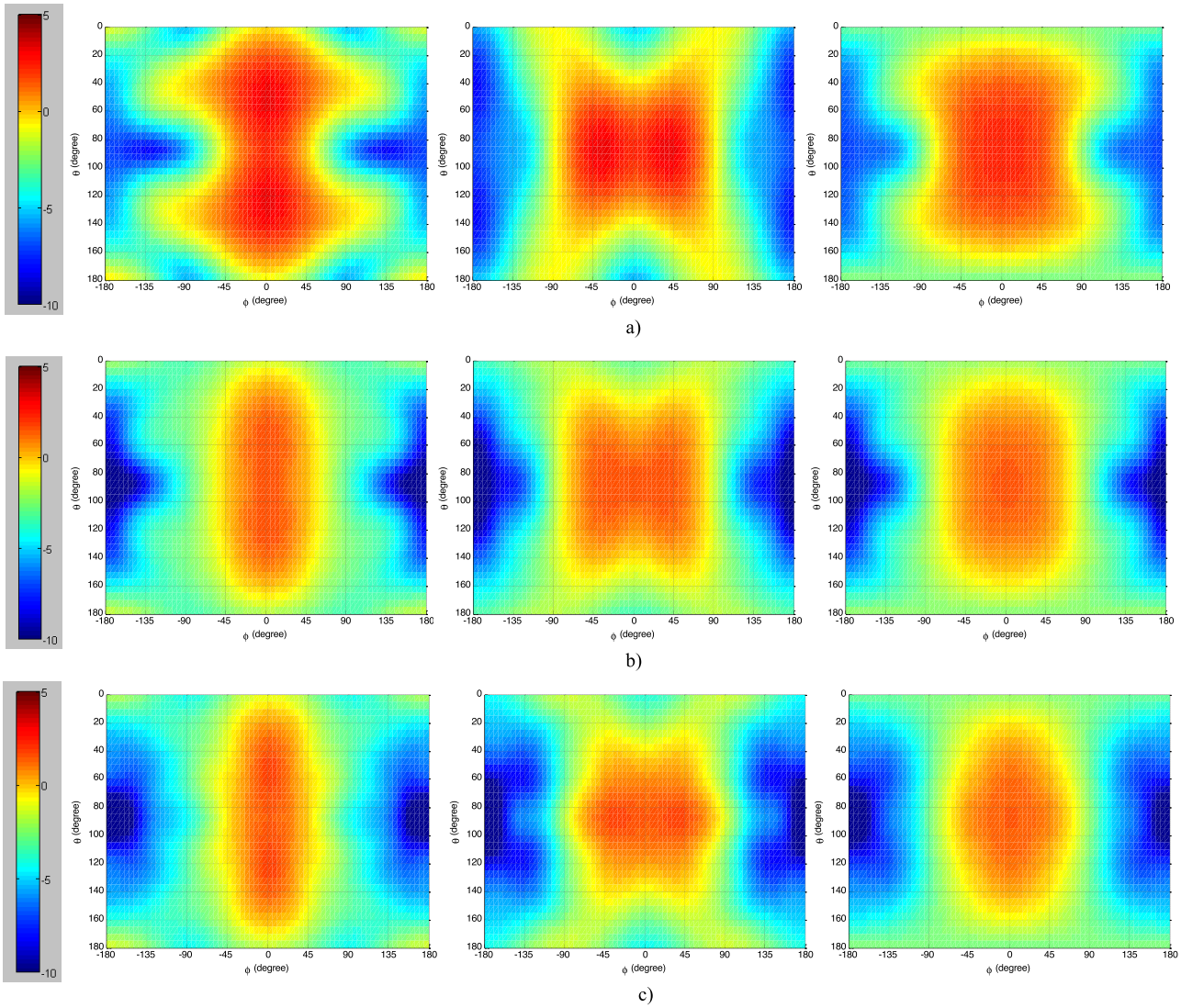

FIGURE 9. 1-bitstream MIMO coverage far field patterns in random-LOS of the 4-port bowtie, corresponding to single incoming wave of vertical polarization (left) and horizontal polarization (middle) and arbitrary polarization (right), (a) 1.7 GHz, (b) 2.2 GHz, and (c) 2.7 GHz. The coverage patterns are obtained by MRC-combining vertical field components of all ports (left) and horizontal field components of all ports (middle), and both vertically and horizontally polarized field components of all ports (right). (a) At 1.7 GHz (Highest directivity of the total MRC pattern: 2.5 dBi). (b) At 2.2 GHz (Higest directivity of the total MRC pattern: 1.8 dBi). (c) at 2.7 GHz (Highest directivity of the total MRC pattern: 1.7 dBi).

scenario in random-LOS. For random-LOS it is impossible to get more than two bitstreams unless we separate the petals by a very large distance, because we cannot generate more than two independent paths between one transmitting and one receiving antenna under pure LOS, i.e. one path corresponding to each of two orthogonal polarizations. We obtain the results for a 2-port bowtie antenna by using the original two orthogonal differential ports of it [19], one for each of the two orthogonal linear polarizations of it, and combining these by using the MRC algorithm. We can do this because each of the differential ports is exciting two opposite petals of the antenna with opposite phase. Note that in random-LOS, the two orthogonal polarizations available will support up to two bitstreams and cannot support more, as already explained. We also see that the PoD curves of the bowties are almost vertical, which is a characteristic of the isotropic 6-port Huygens source [23].

Fig. 8 shows the MIMO 2-stream efficiency versus frequency for the wall-mounted 4-port bowtie antenna in random-LOS. We see that the CP and LP curves are more or less overlapping, and that the 4×2 cases are up to 3 dB lower than the 4×2 i.i.d. cases, due to the correlations between the ports.

The 4-port bowtie antenna has a good MIMO-coverage of the half space (see Fig. 9). Therefore, the PoD slopes of the bowtie antennas in random-LOS are larger than their i.i.d. RIMP counterparts. Nevertheless, due to non-negligible correlations and embedded radiation efficiencies, the MIMO efficiency is smaller than 0 dBiid over most of the frequency range, at 95% PoD.

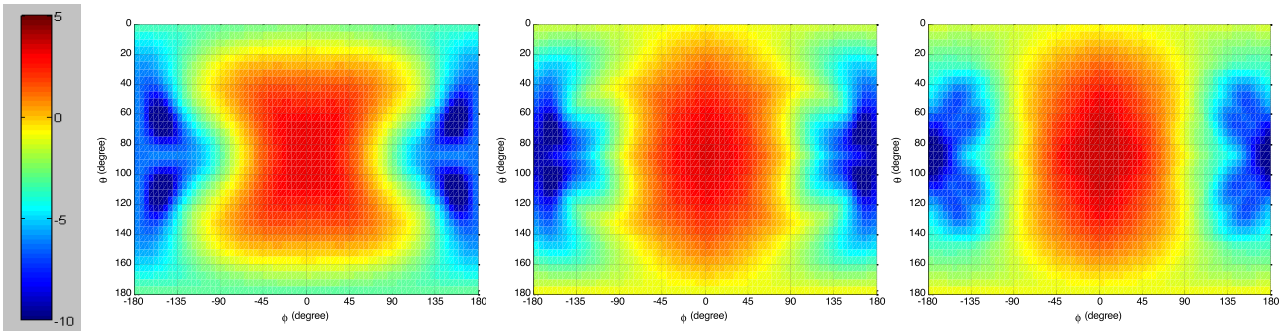

FIGURE 10. 2-stream MIMO coverage patterns of the 4-port bowtie antenna in random-LOS for the wall-mounted scenario at 1.7 GHz (left), 2.2 GHz (middle) and 2.7 GHz (right). (The two incident waves are assumed to be right and left hand circular polarized).

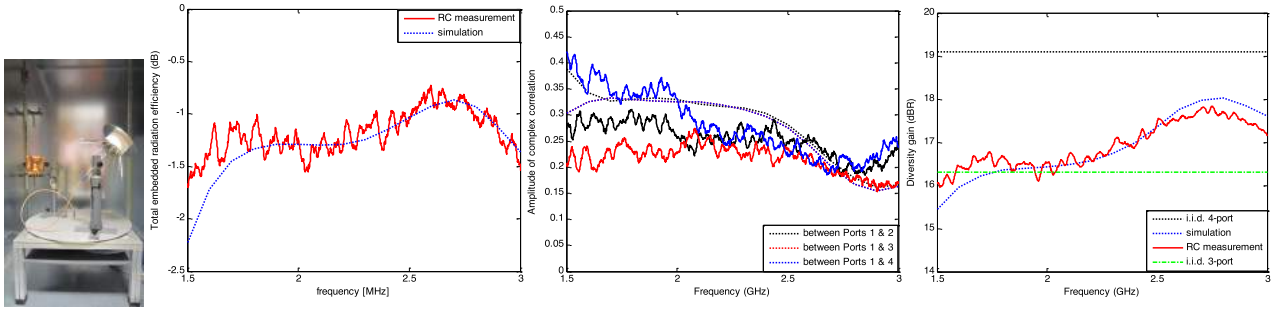

FIGURE 11. Photo of the bowtie antenna during tests in a reverberation chamber. The disk-cone antenna on the right is used for the calibration. The three right graphs show comparisons between simulated results (obtained by CST Microwave Studio and ViRM-lab) and measured results for the 4-port bowtie antenna. a) the total embedded radiation efficiencies on one port (the results are similar on the other prorts); b) the amplitude of the complex correlation between the ports; (c) the effective diversity gains.

E. ANGULAR COVERAGE OF 2- AND 4 BITSTREAMS FOR RANDOM-LOS

We have seen above that the diversity gains and MIMO stream efficiencies of the 4-port bowtie antenna are comparable with the relevant i.i.d. cases over the upper part of the frequency band. In the lower part of the frequency band the results could have been better, which we describe as a physical size limitation with reference to [23]. The bowtie will therefore provide a good angular coverage within the desired hemispherical sector for the wall-mounted case. This coverage quality is ensured by the steep PoD curves. Still, we will here illustrate the quality of the coverage by taking a look at different MIMO coverage radiation patterns, i.e. the far field patterns of the complete MIMO antenna that is present after the channel estimation and the signal MRC or ZF processing in random-LOS.

We present in Fig. 9 a, b and c MIMO coverage far field patterns for the wall-mounted case at three frequencies, respectively. We present three different coverage patterns:

1) The left patterns show the angular coverage of a single bitstream. This is obtained for each angle of incidence by MRC combining the received voltages at all the ports, when an incident linearly-polarized wave of constant amplitude goes through a complete polarization rotation. The MRC means here that the level at each output port from the digital processor is proportional to the MRC combination of the vertical (theta) and horizontal (phi) components of the far fields, and thereafter these MRC combined quantities are MRC-combined with those of the other ports.
2) The middle graphs show the angular coverage of a vertically polarized incoming wave, and the right graphs of a horizontally polarized one. The coordinate system has a vertical z-axis, which means that the vertical polarization is the theta-component, and the horizontal is the phi-component. If both these patterns show good coverage, we know that we can receive two polarizations (i.e. also two bitstreams) with good PoD. Actually, we could also have plotted the combined two-bitstream coverage by using that the PoD of two bitstreams is the same as the PoD of the one with the weakest level (see Fig. 10).

Next, we present in Fig. 10 the 2-stream MIMO coverage patterns of the 4-port bowtie antenna in random-LOS for wall-mounted scenario, at three different frequencies. The ZF receiver is assumed. In each direction, we apply ZF to detect the two circularly polarized orthogonal incident waves (i.e. left and right circularly polarized incident waves). Here we have chosen circularly polarized incident waves, because the coverage patterns turned out to vary with polarization angle if choosing two orthogonal linearly polarized incident waves. The circular polarization case becomes the same as the dual linear polarization case for an arbitrary polarization angle. The minimum value of the ZF output (i.e. the worst stream)

is chosen as the value of the coverage pattern in that direction.

VI. MEASUREMENT IN REVERBERATION CHAMBER

The manufactured bowtie antenna was measured in the Bluetest reverberation chamber (see Fig. 11), and from the results, we obtained the total embedded radiation efficiency, correlation, and diversity gain in RIMP. We see that there is good agreement between the simulations in RIMP and the measurement in reverberation chamber, as expected.

VII. MEASURED FAR FIELD PATTERNS

The measured S-parameters in free space, and the measured embedded radiation efficiencies and correlations in the reverberation chamber are in good agreement with the computed results. We measured also some radiation patterns. We will not give any measured patterns here, but instead refer to [19] where measured differentially-excited patterns are given. There are some disagreements with the simulated patterns, but this is expected because the measurement range is not so good at these low frequencies, and in particular not when measuring antennas with very wide beams.

VIII. CONCLUSION

We have studied the characterization of a wideband 4-port self-grounded bowtie antenna for use in a micro BTS for a MIMO system. This has been done by a completely new approach that never has been published before. Therefore, the emphasis has been to introduce characterizing metrics on MIMO system level, by which we can see the performance for the cases of single as well as multiple bitstreams, for both the two edge environments RIMP and random-LOS. The randomness of the latter is caused by the arbitrary location and orientation of the user with respect to the micro BTS. We have assumed that the BTS antenna is wall-mounted with a desired hemispherical coverage.

The performance in RIMP for the single bitstream case has been characterized in terms of diversity gain. The 4-port bowtie antenna has a diversity gain that is between 1.3 dB and 3 dB lower than the maximum achievable value from a 4-port antenna in RIMP, i.e. from the i.i.d. case. However, the lowest values are very close to the theoretical maximum of an incrementally small multi-port antenna [23]. The theoretical limit for small antennas is a maximum of 6 uncorrelated ports in RIMP and in full-spherical random-LOS. The RIMP limit is in agreement with the ''six distinguishable electric and magnetic states of polarization at a given point, rather than two as is usually assumed'' known from the general Nature paper in [27]. The full-spherical random-LOS limit of maximum six independent co-located ports corresponds to a maximum of 3 ports in half-space (our case). We have also experienced this limitation during the design of the antenna. In order to improve performance we needed to separate the ports and make the antenna larger, which was not desirable in our case.

The performances for the multiple-bitstream cases have been characterized in terms of a MIMO efficiency in dBiid. This is the improvement of the Probability of Detection (PoD) of the specific bitstream being considered, at a 95% PoD level.

The performance of the wideband 4-port example antenna in RIMP shows that we can get two bitstreams with good performance similar to the i.i.d. case. The MIMO 4-stream efficiency is also good at the upper part of the frequency band, but otherwise not, due to the same size-related correlation limitations discussed above for the single bitstream case. At the lower part of the frequency band the degradation is actually very large, so the effect of the correlation is more severe than expected. This should be studied more to get a better understanding of the phenomena.

We have for the first time also designed an antenna for good simultaneous performance in both RIMP and random-LOS. The results for 4 receiving ports in random-LOS show that the diversity gains at 1% CDF are larger than for the corresponding i.i.d. cases. This is possible and not at all unphysical in pure LOS, by the definitions used for the randomness in polarization and AoAs of the single incident wave. Actually, three orthogonal dipoles have a diversity gain of 21.8 dBR in random-LOS, which is 5.5 dB larger than the i.i.d. case [23]. Six Huygens sources have a diversity gain of 24.8 dBR for the full-spherical coverage, which is 2.3 dB larger than the i.i.d. case [23].

The 2-stream performance in random-LOS shows MIMO efficiencies at 90% PoD that is close to what is achievable in RIMP, for the higher part of the frequency band. This is very good for such a small wideband antenna.

The RIMP results were carefully verified by measurements in reverberation chamber. Some far field patterns were also verified by measurements in [19]. We found no need to verify all patterns, because there is very good agreement between simulated and measured S-parameters between the antenna ports in free space, and because of the agreement between simulated and measured correlation and embedded efficiency results for the RIMP case.

It is clear that the performance of the studied antenna could be better, but we were limited by size constraints. This is also the first time anyone tries to optimize for random-LOS, and we are sure that performance of such wideband antennas can be improved in the future when the characterization method has become more mature.

The present characterizations in terms of PoD have never been done before on any practical antenna system, neither in RIMP nor random-LOS. The final results are easy to interpret, and they open up a new world of opportunities for designing and optimizing 5G antennas on system level.

REFERENCES

[1] A. Paulraj, R. Nabar, and D. Gore, *Introduction to Space-Time Wireless Communications*. Cambridge, U.K.: Cambridge Univ. Press, 2003.

[2] M. Barba, ''A high-isolation, wideband and dual-linear polarization patch antenna,'' *IEEE Trans. Antennas Propag.*, vol. 56, no. 5, pp. 1472–1476, May 2008.

[3] F. Gunnarsson *et al.*, "Downtilted base station antennas—A simulation model proposal and impact on HSPA and LTE performance," in *Proc. 68th IEEE VTC Fall*, Sep. 2008, pp. 1–5.
[4] P. C. F. Eggers, J. Toftgård, and A. M. Oprea, "Antenna systems for base station diversity in urban small and micro cells," *IEEE J. Sel. Areas Commun.*, vol. 11, no. 7, pp. 1046–1057, Sep. 1993.
[5] G. R. DeJean, T. T. Thai, S. Nikolaou, and M. M. Tentzeris, "Design and analysis of microstrip bi-Yagi and quad-Yagi antenna arrays for WLAN applications," *IEEE Antennas Wireless Propag. Lett.*, vol. 6, pp. 244–248, 2007.
[6] P.-S. Kildal and K. Rosengren, "Correlation and capacity of MIMO systems and mutual coupling, radiation efficiency, and diversity gain of their antennas: Simulations and measurements in a reverberation chamber," *IEEE Commun. Mag.*, vol. 42, no. 12, pp. 102–112, Dec. 2004.
[7] S. Lu, H. T. Hui, and M. Bialkowski, "Optimizing MIMO channel capacities under the influence of antenna mutual coupling," *IEEE Antennas Wireless Propag. Lett.*, vol. 7, pp. 287–290, Jul. 2008.
[8] P.-S. Kildal and K. Rosengren, "Electromagnetic analysis of effective and apparent diversity gain of two parallel dipoles," *IEEE Antennas Wireless Propag. Lett.*, vol. 2, no. 1, pp. 9–13, Jul. 2003.
[9] K. Rosengren and P.-S. Kildal, "Radiation efficiency, correlation, diversity gain and capacity of a six-monopole antenna array for a MIMO system: Theory, simulation and measurement in reverberation chamber," *IEE Proc. Microw. Antennas Propag.*, vol. 152, no. 1, pp. 7–16, Feb. 2005.
[10] M. V. Ivashina, M. N. M. Kehn, P.-S. Kildal, and R. Maaskant, "Decoupling efficiency of a wideband Vivaldi focal plane array feeding a reflector antenna," *IEEE Trans. Antennas Propag.*, vol. 57, no. 2, pp. 373–382, Feb. 2009.
[11] P.-S. Kildal, C. Orlenius, and J. Carlsson, "OTA testing in multipath of antennas and wireless devices with MIMO and OFDM," *Proc. IEEE*, vol. 100, no. 7, pp. 2145–2157, Jul. 2012.
[12] D. A. Hill, M. T. Ma, A. R. Ondrejka, B. F. Riddle, M. L. Crawford, and R. T. Johnk, "Aperture excitation of electrically large, lossy cavities," *IEEE Trans. Electromagn. Compat.*, vol. 36, no. 3, pp. 169–178, Aug. 1994.
[13] P.-S. Kildal, X. Chen, C. Orlenius, M. Franzén, and C. S. L. Patané, "Characterization of reverberation chambers for OTA measurements of wireless devices: Physical formulations of channel matrix and new uncertainty formula," *IEEE Trans. Antennas Propag.*, vol. 60, no. 8, pp. 3875–3891, Aug. 2012.
[14] P.-S. Kildal *et al.*, "Threshold receiver model for throughput of wireless devices with MIMO and frequency diversity measured in reverberation chamber," *IEEE Antennas Wireless Propag. Lett.*, vol. 10, pp. 1201–1204, Oct. 2011.
[15] P.-S. Kildal and J. Carlsson, "New approach to OTA testing: RIMP and pure-LOS as extreme environments & a hypothesis," in *Proc. EuCAP*, Gothenburg, Sweden, Apr. 2013, pp. 315–318.
[16] P.-S. Kildal, U. Carlberg, and J. Carlsson, "Definition of antenna diversity gain in user-distributed 3D-random line-of-sight," *J. Electromagn. Eng. Sci.*, vol. 13, no. 2, pp. 86–92, Jun. 2013.
[17] J. Yang and A. Kishk, "A novel low-profile compact directional ultra-wideband antenna: The self-grounded bow-tie antenna," *IEEE Trans. Antennas Propag.*, vol. 60, no. 3, pp. 1214–1220, Mar. 2012.
[18] A. Al-Rawi, A. Hussain, J. Yang, M. Franzén, C. Orlenius, and A. A. Kishk, "A new compact wideband MIMO antenna—The double-sided tapered self-grounded monopole array," *IEEE Trans. Antennas Propag.*, vol. 62, no. 6, pp. 3365–3369, Jun. 2014.
[19] H. Raza, A. Hussain, J. Yang, and P.-S. Kildal, "Wideband compact 4-port dual polarized self-grounded bowtie antenna," *IEEE Trans. Antennas Propag.*, vol. 62, no. 9, pp. 4468–4473, Sep. 2014.
[20] U. Carlberg, J. Carlsson, A. Hussain, and P.-S. Kildal, "Ray based multipath simulation tool for studying convergence and estimating ergodic capacity and diversity gain for antennas with given far-field functions," in *Proc. 20th Int. Conf. Appl. Electromagn. Commun. (ICECom)*, Dubrovnik, Kroatia, Sep. 2010, pp. 1–4.
[21] X. Chen, P.-S. Kildal, and M. Gustafsson, "Characterization of implemented algorithm for MIMO spatial multiplexing in reverberation chamber," *IEEE Trans. Antennas Propag.*, vol. 61, no. 8, pp. 4400–4404, Aug. 2013.
[22] P.-S. Kildal, "Rethinking the wireless channel for OTA testing and network optimization by including user statistics: RIMP, pure-LOS, throughput and detection probability," in *Proc. ISAP*, Nanjing, China, Oct. 2013.
[23] P.-S. Kildal and X. Chen, "Fundamental limitations on small multi-beam antennas for MIMO systems," in *Proc. EuCAP*, The Hague, The Netherlands, Apr. 2014.
[24] X. Chen, B. P. Einarsson, and P.-S. Kildal, "Improved MIMO throughput with inverse power allocation—Study using USRP measurement in reverberation chamber," *IEEE Antennas Wireless Propag. Lett.*, vol. 13, pp. 1494–1496, Jul. 2014.
[25] N. Jamaly, P-S. Kildal, and J. Carlsson, "Compact formulas for diversity gain of two-port antennas," *IEEE Antennas Wireless Propag. Lett.*, vol. 9, pp. 970–973, Oct. 2010.
[26] J. Thaysen and K. B. Jakobsen, "Envelope correlation in (N, N) MIMO antenna array from scattering parameters," *Microw. Opt. Technol. Lett.*, vol. 48, no. 5, pp. 832–834, May 2006.
[27] M. R. Andrews, P. P. Mitra, and R. deCarvalho, "Tripling the capacity of wireless communications using electromagnetic polarization," *Nature*, vol. 409, pp. 316–318, Jan. 2001.

PER-SIMON KILDAL (M'76–SM'81–F'95) has been a Professor of Antennas with the Chalmers University of Technology, Gothenburg, Sweden, since 1989, where he is heading the Antenna Group. His main tasks are to lead and supervise research within antenna systems. Until now, he has supervised 21 Ph.D. candidates. He received two Ph.D. degrees from the Norwegian Institute of Technology, Trondheim, Norway.

He has authored over 120 articles in scientific journals; concerning antenna theory, analysis, design, and measurements. Two articles were awarded best paper awards by IEEE. He was a recipient of the prestigious Distinguished Achievements Award from the IEEE Antennas and Propagation Society in 2011.

He has done the electrical design of the 40-m × 120-m cylindrical reflector antenna and line feed of the EISCAT scientific organization, and the dual-reflector Gregorian feed of the 300-m Ø radio telescope in Arecibo. He is the inventor behind technologies, such as dipole with beam forming ring, the hat antenna, and the eleven feed. All these feeds have been used in industry, and until now, over one million hat-fed reflectors have been manufactured for use in radio links. He was the first to introduce the reverberation chamber as an accurate measurement instrument for over-the-air characterization of small antennas and wireless terminals for use in multipath environments with fading. He has also been the originator of the concept of soft and hard surfaces since 1988, today being regarded as the first metamaterials concept. This concept is the basis of his newest and most fundamental invention, the gap waveguide technology. His research is innovative and industrially oriented, and has resulted in several patents and related spinoff companies, the most known being Bluetest AB, Gothenburg.

Prof. Kildal organizes and lectures in courses with the European School of Antenna, Gothenburg. He was the Chairman of the 7th European Conference on Antennas and Propagation in 2013.

XIAOMING CHEN received the B.Sc. degree from Northwestern Polytechnical University, Xi'an, China, in 2006, and the M.Sc. and Ph.D. degrees from the Chalmers University of Technology, Gothenburg, Sweden, in 2007 and 2012, respectively, all in electrical engineering.

He was a Post-Doctoral Researcher with the Department of Signals and Systems, Chalmers University of Technology, from 2012 to 2014. Since 2014, he has been an Antenna Specialist with Qamcom Research and Technology AB, Gothenburg. His research areas include reverberation chamber measurements, MIMO antennas, over-the-air testing, and statistical electromagnetics. He is a reviewer of six IEEE journals.

MATTIAS GUSTAFSSON received the M.Sc. degree from Chalmers University of Technology, Gothenburg, Sweden, in 1998. He is currently with Huawei Technologies Sweden AB, Gothenburg, Sweden, working as an Antenna Specialist. His past career includes 10 years employment at Ericsson AB, Gothenburg, and three years at Cybercom AB, Gothenburg. His main research and development interest is multiantenna systems and their interaction with the wireless channel.

ZHENGZHAO SHEN received the bachelor's degree in telecommunication science and engineering with Northeast University, Shenyang, China, in 1999. He is currently with the Huawei Technologies Wireless Research and Development Center, Shanghai, China, working as a Senior Radio Base Station Architecture Designer. His past career includes 10 more years working at Huawei Technologies, Shenzhen, China, and several years in a small-scale network company. His main research and development interest is multiantenna systems and their interaction with the baseband and radio transceivers and wireless channel.